Middle atmospheric thermal structure obtained from Rayleigh lidar and TIMED/SABER observations: A comparative study

A. Guharay,[1] D. Nath,[2] P. Pant,[1] B. Pande,[3] J. M. Russell III,[4] and K. Pandey[3]

[1]   A novel measurement of seasonal variability of the middle atmospheric thermal structure has been carried out by comparing ground-based lidar and space-based TIMED/SABER observations from a low-latitude station, Gadanki (13.5°N, 79.2°E), India. Lidar temperature has been cross-verified by retrieving from Cooperative Institute for Research in the Atmosphere's (CIRA) CIRA-86 model and SABER observation density and pressure values independently. Observed results are also compared with CIRA-86 model data. Model data show significant difference with observed ones. Observed results match nicely among themselves throughout the year, which further validates the SABER data at low latitude with an average deviation of ∼2 K in 35–75 km altitude range with respect to the Rayleigh lidar. Seasonal pattern of adiabatic lapse rate all over the altitude range reveals a statically stable atmosphere during the observation period. Stratopause temperature shows semiannual oscillation (SAO) in seasonal pattern of variation, which matches with previous observations from low-latitude stations.

Citation: Guharay, A., D. Nath, P. Pant, B. Pande, J. M. Russell III, and K. Pandey (2009), Middle atmospheric thermal structure obtained from Rayleigh lidar and TIMED/SABER observations: A comparative study, *J. Geophys. Res.*, *114*, D18105, doi:10.1029/2009JD011963.

1.   Introduction

[2]   Atmospheric wave activities (wave generation, propagation and interaction with mean wind, etc.) are important for characterization of the thermal structure of the middle atmosphere, and certain chemical reactions contribute to its seasonal variations. Maximum temperature (stratopause) and minimum temperature (mesopause) region demands an extra importance in the context of dynamical perturbations by several means of this unique region. Stratosphere-mesosphere circulation is another significant aspect in view of global scale climate change. For detecting such kind of activities, temperature is a very important parameter for obtaining background structure of the atmosphere and associated perturbations.

[3]   Studies of middle atmospheric thermal structure using various observational methods have been carried out for the last couple of decades by *Leblanc et al.* [1998], *She et al.* [2000], *Taori et al.* [2007], *Guharay et al.* [2008], and *Remsberg et al.* [2008] (hereinafter referred to as R08) with the help of ground-based and space-based observations, but our understanding is not complete still today. Metal resonance lidar can only give temperature profiles in the range of ∼80–100 km because of its own limitation. Among

various probing techniques, Rayleigh lidar is one of the most important. Rayleigh lidar can measure temperatures assuming local thermodynamic equilibrium and hydrostatic equilibrium with reasonably good accuracy within the height range ∼30–80 km [*Hauchecorne and Chanin*, 1980; *Chanin and Hauchecorne*, 1981; *Chanin et al.*, 1985], although the error in calculation of temperatures increases with altitude. Satellite measurements, e.g., Improved Stratospheric and Mesospheric Sounder (ISAMS) and Solar Mesosphere Explorer (SME), have provided significant information of middle atmosphere over a large range of latitudes. Cospar International Reference Atmosphere (CIRA-1986) model [*Fleming et al.*, 1990] gives estimation of seasonal and monthly temperature variations over various latitudes and altitudes, although it lacks important updates according to new experimental results. This shortcoming was corrected by *Clancy and Rusch* [1989], taking into the account of short-term variation. *Namboothiri et al.* [1999] obtained temperature profile of stratosphere and lower-mesosphere region during winter time with Rayleigh lidar from a midlatitude site, Tsukuba, Japan (36°N, 140°E). *Shepherd and Fricke-Begemann* [2004] have shown tidal variability in mesospheric temperature using ground-based potassium lidar and space-based WINDII data over a long period at low- and middle-latitude stations. Middle atmospheric dynamical structure over Gadanki had been investigated by utilizing the lidar data and other existing instruments for the past few years by other investigators. *Venkat Ratnam et al.* [2002] studied mesospheric structure, using coordinated lidar and radar observations. *Nee et al.* [2002] found broad stratopause width (∼10 km) and temperature range of ∼260–270 K

[1]Aryabhatta Research Institute of Observational Sciences, Nainital, India.
[2]National Atmospheric Research Laboratory, Gadanki, India.
[3]Department of Physics, Kumaun University, Nainital, India.
[4]Center for Atmospheric Sciences, Hampton University, Hampton, Virginia, USA.

over Gadanki. Long-term temperature pattern in stratosphere and mesosphere was studied by *Sridharan et al.* [2008], using lidar. *Kishore Kumar et al.* [2008] (hereinafter referred to as KK08) investigated mean background thermal structure of middle atmosphere over Gadanki, using lidar and Sounding of the Atmosphere using Broadband Emission Radiometry (SABER) long-term temperature data and suggested that lidar is very effective to measure nocturnal temperature in the range 35–80 km.

[4] SABER instrument onboard Thermosphere-Ionosphere-Mesosphere Energetics and Dynamics (TIMED) satellite is a suitable one to measure temperature, pressure, density and other parameters, using satellite infrared limb sounding technique with ten channels [*Mertens et al.*, 2001]. Recently, *Xu et al.* [2006] studied MLT region (75–110 km) structure, using sodium lidar and TIMED/SABER comparative observations over a midlatitude station, Colorado, USA (41°N, 105°W). Also from a midlatitude station *Yu and Yi* [2008] derived temperature pattern and associated variability with the help of Raman (3–25 km), Rayleigh (25–75 km) and Fe Boltzmann (80–105 km) lidar measurements. They found good agreement with radiosonde, satellite, and model data. Comparison between SABER and other studies gives good insight about the present understanding of the non local thermodynamic equilibrium (LTE) processes. *Mertens et al.* [2004] showed comparison between SABER-derived (version 1.02) temperature and falling sphere (FS) measurement from Andøya, Norway (69°N, 16°E), at thermospheric altitudes. They obtained good agreement in some altitude ranges, while they observed significant difference between results obtained from the two observational methods at some other ranges. The most recent work by *Mertens et al.* [2009] has shown fairly good agreement between SABER version 1.06 temperature, rocket falling sphere and lidar data from middle- (Colorado) and high-latitude (Andøya) stations. It is also observed from their comparison study that SABER version 1.04 and version 1.06 data do not show any significant change. The latest algorithm (version 1.07) of SABER temperature is expected to provide better agreement with other observations owing to significant modification (R08) in the retrieval techniques by reducing the earlier drawbacks.

[5] Very few studies have been done so far from low-latitude stations with rocket observations [e.g., *Chakravarty et al.*, 1992; *Mohanakumar*, 1994] and ground-based lidar observations [e.g., *Siva Kumar et al.*, 2003] (hereinafter referred to as SK03) [see also *Venkat Ratnam et al.*, 2002; *Parameswaran et al.*, 2000; *Nee et al.*, 2002; *Kishore Kumar et al.*, 2008]. Our aim in this present paper is to study the seasonal thermal structure of stratosphere-mesosphere system from a low-latitude station, Gadanki (13.5°N, 79.2°E) and additional validation of TIMED/SABER temperature data by ground-based Rayleigh lidar and satellite-based data in the year 2006. We have also compared our results with CIRA-1986 model data.

## 2. Instruments Used for the Observations

2.1. Lidar

[6] The lidar at National Atmospheric Research Laboratory (NARL) consists of a laser pulse transmitter, two telescope system for receiving backscattered light, data acquisition and processing system. It utilizes Nd:YAG laser as a source with an average energy of 550 mJ per pulse at second harmonic ~532 nm. The lidar operates at a pulse repetition frequency of 20 Hz and a pulse width of 7 ns. A beam expander is used to expand the beam 10 times to reduce the beam divergence from 0.45 mrad to 0.1 mrad. A narrow band interference filter (FWHM ~ 1.07 nm) is used to reduce backscattered noise from the actual signal. Two receivers are used to receive the Rayleigh and Mie back-scattered signal. The Rayleigh receiver consists of a 75 cm Newtonian telescope for atmospheric density and temperature estimation and the Mie receiver consists of a 35 cm Schmidt-Cassegrain telescope for aerosol and cloud studies. The Rayleigh receiver has a field of view of ~1 mrad. The detector of the lidar system consists of two channels, using two identical Photo Multiplier Tube (PMT) set at different gains (9:1) to increase the dynamic range of the detector. The low-sensitivity channel (U channel) is set for high backscattered signal intensity from 30 to 50 km altitude range. The high-sensitivity channel (R channel) is meant for comparatively low incoming signal strength from the range 50–80 km. The PMTs are operated in photon counting mode and the outputs of the PMTs are fed into two pulse discriminators, which contain 300 MHz pulse amplifier. Outputs of the discriminators are passed to a PC-based photon counting data acquisition system. It is operated by a multi channel scalar (MCS) software, which gives out photon profiles with 300 m range resolution and 250 s time resolution after integrating 5000 laser shots. The details of the instrument are given elsewhere [e.g., *Bhavani Kumar et al.*, 2000].

[7] The temperature is calculated from the photon count profiles, using the algorithm that is almost same as the method given by *Hauchecorne and Chanin* [1980]. In the height range >30 km, where contamination in estimating temperature owing to Mie contribution is negligible, the backscattered intensity (corrected for range and atmospheric transmission) is proportional to molecular number density. Using the number density from a standard model (CIRA-86) at around ~50 km, where signal-to-noise ratio is very high, the density profile for all the height range (30–90 km) is calculated. Pressure profile is computed from the obtained density profile, assuming hydrostatic equilibrium (pressure is proportional to density) by taking pressure value from CIRA-86 model at 90 km. At last the temperature profile is calculated from the number density and pressure profiles assuming ideal gas law. The details of the data analysis method of the lidar data are given by SK03. In our paper we have used lidar data of 111 nights of the year 2006.

2.2. SABER

[8] TIMED satellite is at an altitude of 625 km above ground level with inclination of about 74.1° from the equator and its orbital period is ~97 min. SABER, one of the four instruments placed onboard the TIMED satellite is a radiometer, which measures infrared emissions from 1.27 μm to 15.2 μm [*Russell et al.*, 1999] from lower stratosphere to lower thermosphere at 15 longitudes each day and on each orbit. These emissions are from carbon dioxide, ozone, nitric oxide, water vapor, molecular oxygen
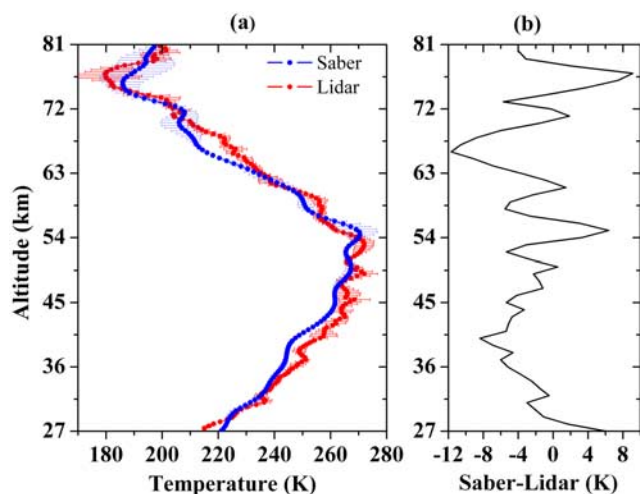
Figure 1. (a) A typical nocturnal profile of temperature of lidar (2030 LT, 30 January 2006 to 0150 LT, 31 January 2006) and SABER (~2230 LT) and (b) the difference (SABER-lidar) of two profiles on 30 January 2006. A total of 81 soundings for lidar and 2 soundings for SABER (at $10-16°N$ and $73-85°E$) are used to derive the profiles. Horizontal bars show standard deviations of means.

and hydroxyl. It covers a latitude range of 54°S to 82°N or 82°S to 54°N depending upon TIMED yaw cycle (yaw cycle ~ 60 days). The TIMED orbit is quasi sun synchronous. Its orbital precession is such that local time varies day to day and in about 60 days, complete local time coverage is obtained. Details of the temperature calculation and consideration of non-LTE radiative transfer in retrieval algorithm of the temperature computation are given by *Mertens et al.* [2001]. Recently R08 have shown the validation results of SABER v1.07 data with other ground-based and satellite-based measurements. The main sources of errors in SABER are found to be due to inaccuracy in measured irradiance, biases in the forward model of CO_2 radiance, errors due to ozone and uncertainties in retrieved temperature profiles with respect to reference pressures. They have also mentioned that the uncertainty is on the order of $1-3$ K in lower stratosphere, ~1 K near stratopause and around ~2 K in mesosphere and lower thermosphere and hence it is suggested that the SABER can be utilized to determine diurnal-interannual-scale temperatures especially for upper mesosphere and lower-thermosphere region.

[9] Previous comparative study, using meteor trail decay time to derive temperature and SABER observation in mesopause region by *Kumar* [2007] from an equatorial site, Thumba, India (8.5°N, 77°E) revealed very interesting results, which has urged the need of collocated studies for acquiring better clarification. Our present study has tried to minimize the underlying gap regarding middle atmosphere and provide cross verification utilizing comparative lidar and SABER observations. In our present study we have used SABER version 1.07, level2A data set for analysis. The data are obtained from http://saber.gats-inc.com./ website. We have used 284 nights of data for the year 2006 within the latitude range $10-16°N$ and longitude range $73-$

85°E centered about our observation location, Gadanki, India (13.5°N, 79.2°E).

3. Results and Discussions

[10] In our current work, we would like to show additional SABER v1.07 temperature validation from a low-latitude station as well as the seasonal characteristics of middle atmospheric thermodynamical structure and related variability with the help of Rayleigh lidar and TIMED/SABER data for the year 2006.

3.1. Comparison of Lidar and SABER

[11] Figure 1a shows typical nocturnal mean temperature profile within the height range 27–80 km of lidar (using 81 vertical profiles of total 5 h 20 min observational duration started at 2030 LT) and SABER (of 2 vertical profiles obtained at ~2230 LT with 36-s interval) on 30 January 2006. Both profiles show steady variation of temperature with altitude and the small scale variability is embedded on them. They also delineate good agreement. The small scale variability is probably due to the wave activities (gravity waves and tides). Observed stratopause is around $53-55$ km with a mean temperature on the order of ~271 K. Figure 1b shows the height profile of the temperature difference between the SABER and the lidar. The difference is on the order of maximum $\sim\pm11$ K. The SABER temperature is colder than the lidar one of maximum around ~11 K at 66 km height, and the SABER is hotter than the lidar of maximum around ~9 K at 77 km. The mismatch between the two profiles is possibly due to broad SABER latitude $(10-16°N)$, longitude $(73-85°E)$ range selection for the present study or may be due to imperfect coincidence of the two observations or the assumptions made in deriving the temperatures.

[12] Further, to assess the effect of the assuming model (CIRA-86) density at 50 km and the pressure at 90 km in retrieving the lidar temperature profiles, we have replaced (1) density at 50 km, (2) pressure at 90 km, and (3) both density at 50 km and pressure at 90 km, by the SABER observed values to re-determine 30 January temperature profile. The obtained profiles are shown in Figure 2. It is evident from the plot that all the profiles track very well each other. One important point is to be noted that significant similarity exists among all the profiles with a maximum bias of ~3 K. It is concluded from the perturbations to the model values that there is very little uncertainty in the retrieved lidar temperatures. Detailed description of assumed model density and pressure values on the derived lidar temperature was discussed previously from the same observational site by SK03, using CIRA-86 and MSISE-90 models.

[13] Figure 3a shows monthly average temperature profiles of the individual nights for the month of February with lidar as well as SABER data. CIRA-86 model data are also plotted along with those for comparison. The horizontal bars represent the standard deviations, which are actually measure of monthly variability for both lidar and SABER. It is clear from the plot that variability increases with altitude owing to geophysical variability and it has a maximum of ~15 K for lidar at ~80 km altitude. It is noteworthy to say that lidar and SABER temperatures match nicely, while
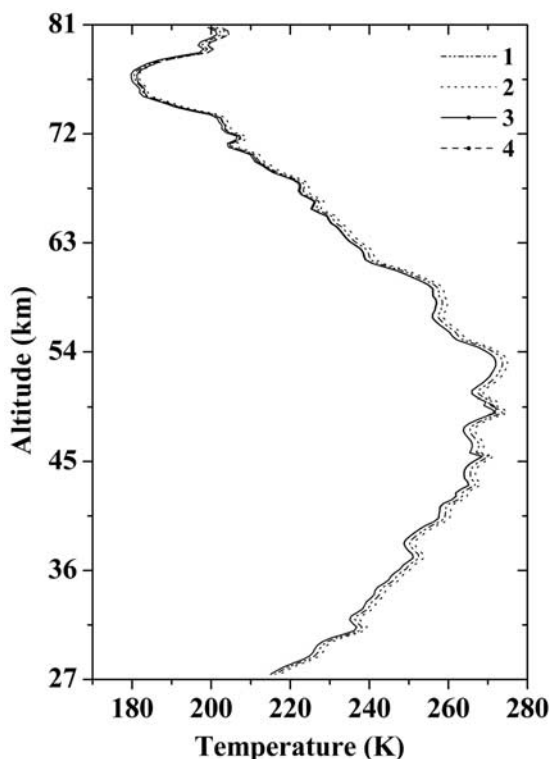
Figure 2. Retrieved lidar temperature profiles of 30 January 2006 by assuming (1) SABER density at 50 km and pressure at 90 km, (2) SABER pressure at 90 km, (3) CIRA-86 density at 50 km and pressure at 90 km, and (4) SABER density at 50 km.

CIRA-86 model temperature shows significant difference with the other two around ∼50 km and above ∼63 km altitude, and in most of the range it is higher than other two profiles. It is interesting to see that above ∼30 km the lidar and the SABER profiles vary well inside their observed range of standard deviations. From Figure 3b it is evident that magnitude of difference between the SABER and the lidar monthly average temperatures is much less (±5 K) than the daily profile shown in Figure 1.

[14] The differences between the CIRA-86 (at 15°N) model and the observed values are due to several reasons. CIRA has very poor vertical as well as horizontal resolution, which gives error in estimation of the observed temperature. CIRA model cannot accurately measure the temperature for the case of seasonal transition, e.g., summer to autumn, autumn to winter, etc. [*Leblanc et al.*, 1998], and regional atmospheric changes owing to sudden stratospheric warming or mesospheric cooling, etc. [*Manson et al.*, 2008]. Semiannual oscillation (SAO) in mesospheric region might be another reason of mismatch as SAO is not considered in CIRA model and this type of disagreement was also observed by *Clancy et al.* [1994] in comparison with SME global temperature data. It should also be noted that CIRA model estimate is based on rocket data of 1960s and satellite data of 1970s and by the time of our observation, significant cooling [*Dunkerton et al.*, 1998] of the middle atmosphere has taken place, which adds additional error in the CIRA temperature estimates. Hence accuracy of the CIRA model reduces as the time goes on. Better agreement between the monthly average profiles of the lidar and the SABER is due to long-term average (smoothing) of the both.

3.2. Seasonal Characteristics Observed From Lidar and SABER

[15] For characterizing seasonal behavior, average profiles of the middle atmospheric thermal structure have been shown in Figure 4, using four different seasons considering Summer (May, June, July, and August), Autumn (September and October), Winter (November, December, January, and February) and Spring (March and April). The horizontal bars represent standard deviations of the respective profiles. It is interesting to see that both (lidar and SABER) the profiles track well each other within the standard deviations except below ∼35 km. Another point is to be noted that comparatively large difference is found in the autumn season profiles below ∼35 km.

[16] Difference of the two profiles in the upper mesospheric region (>72 km) may be due to the lack of fulfillment of the thermodynamic conditions (model pressure at 90 km for retrieving temperature of lidar, uncertainty because of errors owing to non-LTE radiative transfer correction in SABER temperature calculation, etc.) presumed for the retrieval of the temperature for lidar (SK03) or SABER [*Mertens et al.*, 2004] individually or both. Another important reason for such anomaly may be tidal activity, which is significant in low-latitude mesosphere and reflects in our results. In this context, it can be mentioned that *Mertens et al.* [2009] found the difference (SABER-lidar) temperature of ∼20 K at 90 km altitude from Fort Collins, Colorado. Significantly lower temperature of the lidar profiles compared to the SABER ones in the lower altitude (<35 km) for all the seasons may be due to the nonlinearity of the detector at low altitude because of high backscattered signal, which is known as pulse pileup [*Donovan et al.*, 1993]. Recently, KK08 mentioned that the temperature data of the Gadanki lidar below 35 km contains considerable uncertainty. The observed higher-
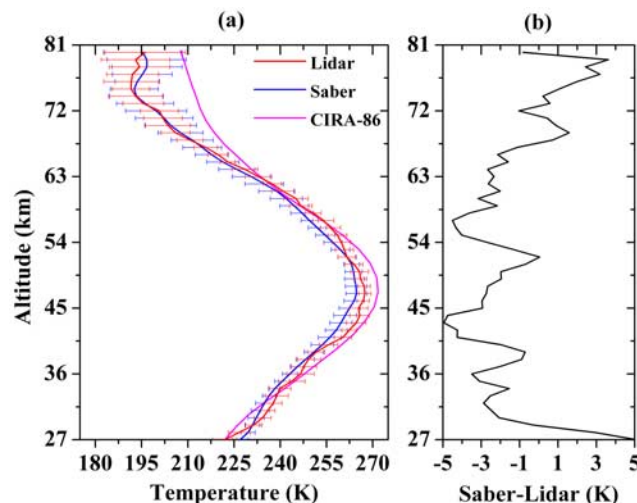
Figure 3. (a) Monthly average profiles of temperature of lidar and SABER for February 2006 along with CIRA-86 model data. Horizontal bars are representing standard deviations of monthly temperatures (b) Deviation temperatures (SABER-lidar).
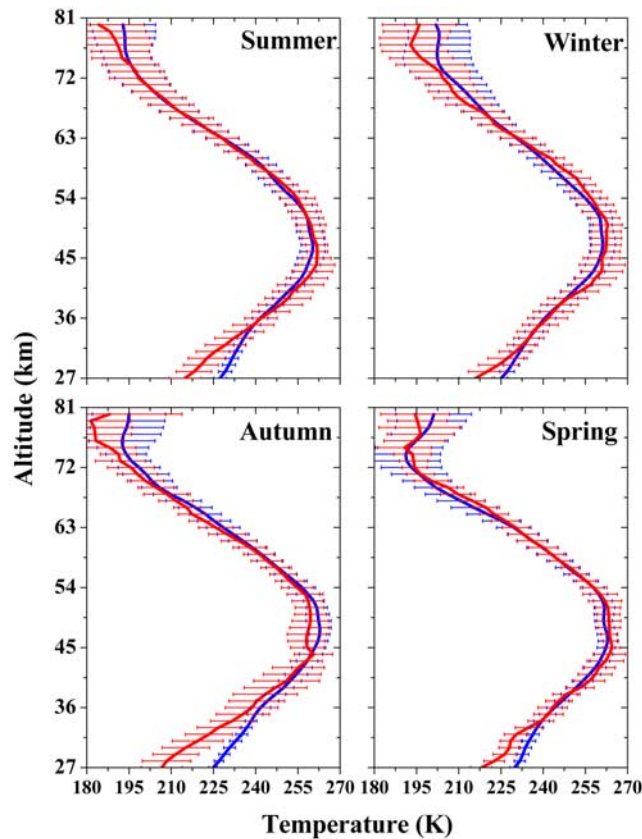
Figure 4. Seasonal average profiles of summer, winter, autumn, and spring (details are given in section 3.2) with standard deviations of lidar (red) and SABER (blue).

profiles of the same of the SABER and the lidar for all the altitude range. The distinction obtained from these two observations, varies mostly within the range $\sim\pm10$ K (except below 42 km during the month of June and October, when the deviation is comparatively higher). Observed higher variability (standard deviation) of the lidar mean temperature during June and September may be due to contamination by the extant clouds on few days in monsoon. The most recent study of KK08 indicates very good agreement between the Gadanki lidar and the SABER long-term observations with maximum deviation on the order of ~4 K in 35–80 km altitude range. R08 showed the comparison of the SABER-derived and the Rayleigh lidar temperature from a low-latitude station, Mauna Loa (20°N) in the range $\sim20-100$ km with yearly average data of the years 2002–2005. They found deviation (SABER-lidar) temperature $\sim1-3$ K below 40 km and above 80 km the SABER is hotter than the lidar most of the time. Our seasonal average vertical temperature difference of the same (not shown here) shows variability of $\sim\pm2$ K in the altitude range $\sim35-75$ km, which validates the SABER-derived temperature well within this range.

3.3. Stability Condition

[18] Adiabatic lapse rate (ALR $\sim$ dT/dz) is an important parameter to determine the static stability of the atmosphere. If an air parcel ascends through the atmosphere, the parcel will expand adiabatically (no exchange of energy between
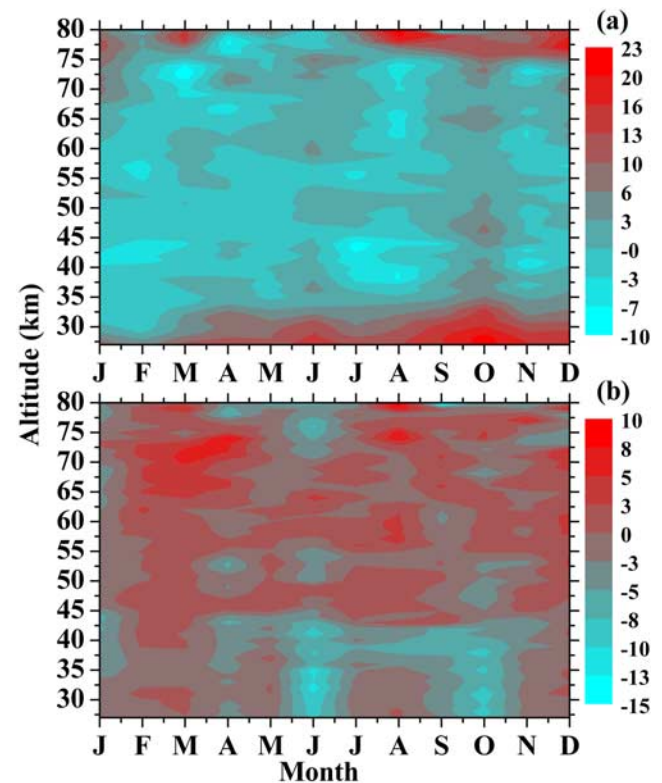
temperature difference below 35 km in the autumn season compared with the other ones is possibly due to least coincidence of the lidar and the SABER observation durations used for the present analysis, which has worse effects at lower altitudes owing to lidar inefficiency as described before or may be some unknown temporary fault persisted to the lidar system. In addition to the discussed mismatches, it should be remembered that the SABER vertical profiles are derived by integrating over few seconds and lidar profiles are obtained by nightly integration (few hours), which can cause further disagreement in all the profiles throughout the year.

[17] Figure 5a describes the seasonal pattern of difference (SABER-lidar) of monthly average temperature profiles. It is conspicuous from the contour plot that most of the time below 35 km the SABER temperatures are higher than the lidar ones. In the altitude range above 35 km, the lidar temperatures are generally greater than the SABER in first half of the year. It is noteworthy to say that during October the SABER temperatures are significantly higher at all altitudes with a maximum up to $\sim20-23$ K below 30 km. Most prominently, the lidar temperatures are a maximum of ~10 K higher than the SABER at altitude 40–45 km during the July–August period. Overall, it is observed that most of the time deviations are of ~10 K except few events described before, which justifies good agreement between the lidar and the SABER observations. Figure 5b depicts the difference of standard deviations of the monthly average

Figure 5. Seasonal pattern of difference (SABER-lidar) of (a) monthly average temperature profiles of lidar and SABER shown in the contour and (b) corresponding difference of standard deviations of SABER means and lidar means.
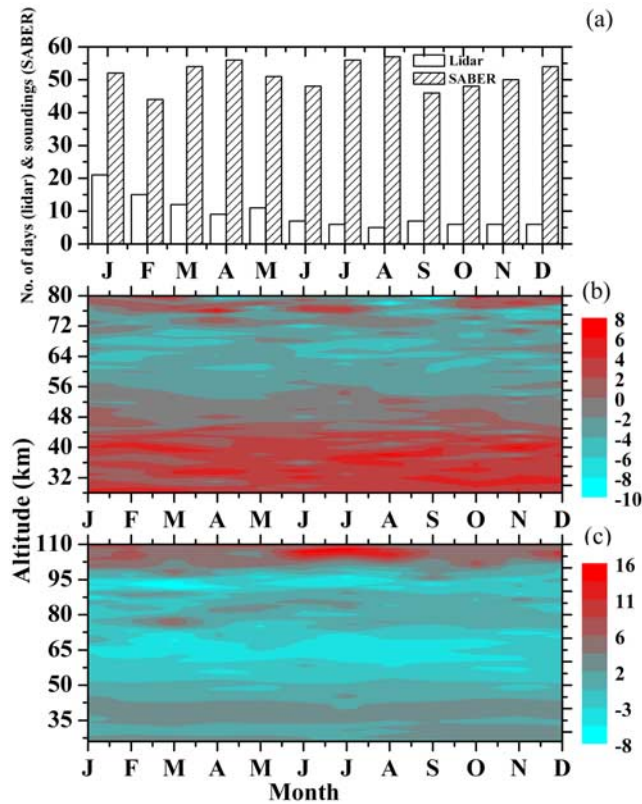
Figure 6. (a) Monthly statistics of total number of soundings of SABER and days of observation of lidar of the year 2006. The adiabatic lapse rate over the year 2006 is shown in the contours for (b) lidar and (c) SABER.

the air parcel and the surrounding) as pressure decreases with altitude and hence its temperature will decrease owing to adiabatic cooling. When it descends, its temperature increases owing to adiabatic heating. Static stability is defined as

$$S = \left(\frac{dT}{dz}\right) + \Gamma \qquad (1)$$

where dT is increase (decrease) of temperature owing to a range of dz altitude increase (decrease). Γ is dry adiabatic lapse rate. The value of Γ is $\sim 10°$ K/km. Atmosphere is statically stable if $S > 0$, and there is no vertical mixing of air parcels owing to convection process. If $S < 0$ then atmosphere is unstable against convection and there will be transport of heat to get the value of S near to zero. Hence from the above discussion it is evident that if ALR is less than $-10°$K/km then the atmosphere will be convectively unstable. We have calculated ALR for the whole year 2006, using monthly averaged individual temperature profile for altitude range 28–80 km for lidar and 26–110 km for SABER to find out the atmospheric stability condition during the observation period in Figure 6.

[19] Observation data statistics has been shown in Figure 6a of total number of soundings and days of observations in each month of the year for SABER and lidar. Lidar observation provides good temporal coverage of the observing nights,

whereas SABER achieves consistent soundings of the concerned months throughout the year. Wintertime observation is quite high for lidar in comparison with other seasons because of clear weather condition. We found SABER profiles with our designated, latitude/longitude grid for about 18 days per month round the year with reasonable soundings as depicted by the plot.

[20] Figures 6b and 6c depict the lidar and SABER derived adiabatic lapse rate, respectively. Evident from the two plots is that S is always >0. The maximum range of variability of ALR is within -10 to $+16$. SABER derived ALR has revealed lower variability. One important point to be noted is that most of the time, atmosphere of altitude below 45 km is highly stable. The mesopause region (near 80 km) possesses high stability during some periods of the year. Above 105 km (turbopause) the region is extremely stable as evident from the SABER contour throughout the season. Both contours match close to each other. It is well known that the stratosphere is under radiative equilibrium and hence it is almost stable most of the time. In this context, it should be mentioned that *Kiehl and Solomon* [1986] discussed very nicely, regarding the stratospheric radiative balance and indicated high possibility of the stratosphere to be in radiative equilibrium. Later on *Mlynczak et al.* [1999] showed that the stratosphere is in global mean radiative equilibrium on monthly timescales and it was also found that in the mesosphere the chemical heating rates owing to several exothermic reactions exceed the solar heating rates, which implies the equilibrium to be unlikely there. After advent of the SABER instrument, extensive study of mesospheric radiative balance/imbalance has become possible owing to adequate data, but still significant study is required to obtain the understanding of the radiative condition of this least explored region. Although our interpretation of stability is limited by spatial and temporal extent in terms of long-term average for SABER and lidar, respectively, the unstable regions are of significant interest because of causative mechanisms, e.g., gravity waves and tidal activities.

3.4. Stratopause Variability and SAO

[21] Figure 7 shows the stratopause variation characteristics throughout the year 2006 over Gadanki. Figures 7a and 7b show monthly average stratopause height and temperature variation, respectively, for both lidar and SABER observations, and vertical bars represent monthly standard deviations. Stratopause height varies in the range 44–51 km all through the year with generally ± 5 km variability except during fall equinox in case of lidar, when variability is quite high. Stratopause temperatures also show significant variability of ~ 260–270 K, which is similar to the previous observation result of *Nee et al.* [2002] from Gadanki during 1998–1999. Lidar derived stratopause height is always lower than the SABER one except during October and the opposite phenomenon is observed in case of stratopause temperatures, where the SABER is always lower than the lidar except October. No clear signature of semiannual oscillation (SAO) is observed in the stratopause height, while it is evident in the temperature pattern for both lidar and SABER with its maxima around equinox and minima around summer and winter (SK03; KK08). Our observed stratopause heights are almost in opposite phase
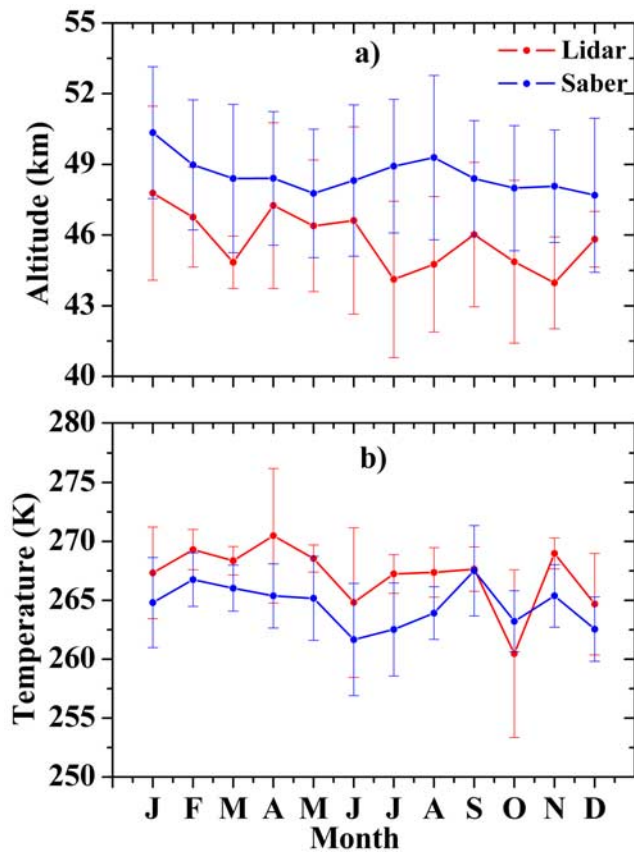
Figure 7. Seasonal plot of monthly mean (a) stratopause height and (b) stratopause temperature.

with stratopause temperatures for both Lidar and SABER. Also few other investigators [e.g., *Mohanakumar*, 1994; *Kishore Kumar et al.*, 2008] showed SAO in stratopause temperature and heights from Indian low-latitude regions in the past.

[22] SAO is an important feature of stratosphere-mesosphere region, which is mainly caused by interaction of gravity waves, tides generated primarily owing to strong convection in the lower atmosphere of tropical regions. This event was also reported by several investigators in the last few decades through observational and theoretical studies. *Garcia et al.* [1997] examined apparent modulation of stratospheric SAO by the quasi-biennial oscillation (QBO) in the rocketsonde data and also their subsequent observations of high-resolution Doppler imager (HRDI) and medium-frequency (MF) radar data revealed a correlation between easterly phase of SAO and QBO. There is a high possibility of our observed SAO is effected by QBO, but we can't conclude it absolutely because of limited duration of observation. Stratopause SAO also plays an important role in generation of mesosphere semiannual oscillation (MSAO) by selective transmission of gravity and Kelvin waves through itself [*Dunkerton*, 1982]. Recently, *Ratnam et al.* [2008] investigated the effect of stratospheric QBO (SQBO) on MSAO and MQBO and they also found strong influence of MQBO on MSAO owing to nonlinear interaction. It is important to mention that the best sinusoidal fit to our data similar to *Guharay et al.* [2008] of period 6 month

has revealed amplitude of 0.7 and 1.8 K for lidar and SABER, respectively. This is a bit smaller than the comparison range of SAO amplitude (2.1–5.8 K) among various investigators' results obtained from the subtropical regions (latitude range ∼20–23°), as shown by *Zhao et al.* [2007]. Most recent observation from the same site (Gadanki, India) by *Sridharan et al.* [2008], using long-term (1998–2008) temperature data of Rayleigh lidar has revealed SAO amplitude on the order of ∼1 K in 40–55 km altitude region, which lies well within our observed range. Low value of the SAO amplitude as comes out from our study may be because of complex wave interaction, e.g., Rossby-gravity wave, Kelvin waves, tides, etc., which reduces the SAO amplitude to some extent. These waves are very important entities of modifying equatorial dynamics and hence our study implies the need of further investigations to unveil these hidden features. It was mentioned before that the lidar and SABER temperature profiles are obtained by nightly (few hours) and few seconds' average, respectively. Stratopause variability is shown after performing whole month average of the nightly profiles of both observations. Hence tidal aliasing is present in both data owing to long-term average, and that affects the SAO component to be observed in stratopause height and temperature. Also during the observation, the SABER local ascending and descending, orbital observation times undergo precession of few hours in monthly time scales. This tidal aliasing may subdue the expected SAO feature in the stratopause height variability.

4. Conclusions

[23] Present comparative observational study is carried out from a low-latitude station, Gadanki (13.5°N, 79.2°E) for additional validation of SABER temperature retrieval from an equatorial station and determine thermal structure of the middle atmosphere (27–80 km) with the help of ground-based lidar and space-based TIMED/SABER data. Observed results are also compared with existing CIRA-86 model. From the above study it is inferred that the observational results show significant difference with the model. Hence the model is to be corrected, taking into account several small and large scale middle atmospheric wave activities, which are contributing in myriad way to the thermal energy budget and variability. Good agreement between these two instruments' measurement has provided additional validation of the SABER temperature at low latitude. Observations done by lidar and SABER have revealed statically stable atmosphere (mainly stratosphere) throughout the year, although there are few unstable regions, probably due to the atmospheric wave activities. SAO has been observed in stratopause temperature pattern, though it is not prominent in stratopause height variation profile. Similarity between the ground-based and space-based observation during most of the time justifies them to be good complementary methods for middle atmospheric probing. At the same time, small disagreement between these two is mainly due to the lack of spatial coincidence of the observations and difference in time integration in deriving each day temperature profile and finally retrieval algorithm used to derive temperatures for these two observing techniques. As it is already mentioned that observations

from tropical region is still lacking, hence our study carries its own importance for unveiling characteristics of this unique atmospheric region. Previously, KK08 carried out good comparative study of middle atmospheric thermal structure over Gadanki, using lidar and SABER temperature data, but the exploration of the stability condition of this region was untouched and it is incorporated in our study to provide more insights. Diurnal and semidiurnal tides, which are other important contributors to the middle atmospheric variability in low-latitude region [*Marsh et al.*, 2006], and not explored in the present research work, require further investigations. Hence, more observational studies are to be performed to gain complete knowledge associated with the processes prevailing there.

References

Bhavani Kumar, Y., V. Siva Kumar, P. B. Rao, M. Krishnaiah, K. Mizutani, T. Aoki, M. Yasui, and T. Itabe (2000), Middle atmospheric temperature measurements using ground based instrument at a low latitude, *Indian J. Radio Space Phys.*, *29*, 249–257.

Chakravarty, S. C., J. Datta, and C. P. Revankar (1992), Climatology of longperiod oscillations in the equatorial middle atmosphere over Thumba, India, *Curr. Sci.*, *63*, 33–42.

Chanin, M.-L., and A. Hauchecorne (1981), Lidar observation of gravity and tidal waves in the stratosphere and mesosphere, *J. Geophys. Res.*, *86*, 9715–9721, doi:10.1029/JC086iC10p09715.

Chanin, M.-L., A. Hauchecorne, and N. Smires (1985), Contribution to the CIRA model from ground based lidar, in *Handbook for MAP*, vol. 16, pp. 305–314, Middle Atmos. Program, Int. Counc. of Sci. Unions, Paris.

Clancy, R. T., and D. W. Rusch (1989), Climatology and trends of mesospheric (59–90 km) temperatures based upon 1982–1986 SME limb scattering profiles, *J. Geophys. Res.*, *94*, 3377–3393, doi:10.1029/JD094iD03p03377.

Clancy, R. T., D. W. Rusch, and M. T. Callan (1994), Temperature minima in the average thermal structure of the middle atmosphere (70–80 km) from analysis of 40- to 92-km SME global temperature profiles, *J. Geophys. Res.*, *99*, 19,001–19,020, doi:10.1029/94JD01681.

Donovan, D. P., J. A. Whiteway, and A. I. Carswell (1993), Correction for nonlinear photon-counting effects in lidar systems, *Appl. Opt.*, *32*, 6742–6753, doi:10.1364/AO.32.006742.

Dunkerton, T. J. (1982), Theory of the mesopause semiannual oscillation, *J. Atmos. Sci.*, *39*, 2681–2690, doi:10.1175/1520-0469(1982)039<2681:TOTMSO>2.0.CO;2.

Dunkerton, T. J., D. P. Delisi, and M. P. Baldwin (1998), Middle atmosphere cooling trend in historical rocketsonde data, *Geophys. Res. Lett.*, *25*, 3371–3374, doi:10.1029/98GL02385.

Fleming, E. L., S. Chandra, J. J. Barnett, and M. Corney (1990), Zonal mean temperature, pressure, zonal wind and geopotential height as functions of latitude, *Adv. Space Res.*, *10*(12), 11–59, doi:10.1016/0273-1177(90)90386-E.

Garcia, R. R., T. J. Dunkerton, R. S. Lieberman, and R. A. Vincent (1997), Climatology of the semiannual oscillation of the tropical middle atmosphere, *J. Geophys. Res.*, *102*, 26,019–26,032, doi:10.1029/97JD00207.

Guharay, A., A. Taori, and M. Taylor (2008), Summer-time nocturnal wave characteristics in mesospheric OH and O_2 airglow emissions, *Earth Planets Space*, *60*, 973–979.

Hauchecorne, A., and M.-L. Chanin (1980), Density and temperature profiles obtained by lidar between 30 and 70 km, *Geophys. Res. Lett.*, *7*, 565–568, doi:10.1029/GL007i008p00565.

Kiehl, J. T., and S. Solomon (1986), On the radiative balance of the stratosphere, *J. Atmos. Sci.*, *43*, 1525–1534, doi:10.1175/1520-0469(1986)043<1525:OTRBOT>2.0.CO;2.

Kishore Kumar, G., M. Venkat Ratnam, A. K. Patra, S. Vijaya Bhaskara Rao, and J. Russell (2008), Mean thermal structure of the low-latitude middle atmosphere studied using Gadanki Rayleigh lidar, Rocket, and SABER/TIMED observations, *J. Geophys. Res.*, *113*, D23106, doi:10.1029/2008JD010511.

Kumar, K. K. (2007), Temperature profiles in the MLT region using radar-meteor trail decay times: Comparison with TIMED/SABER observations, *Geophys. Res. Lett.*, *34*, L16811, doi:10.1029/2007GL030704.

Leblanc, T., I. S. McDermid, P. Keckhut, A. Hauchecorne, C. Y. She, and D. A. Krueger (1998), Temperature climatology of the middle atmosphere from long-term lidar measurements at middle and low latitudes, *J. Geophys. Res.*, *103*, 17,191–17,204, doi:10.1029/98JD01347.

Manson, A. H., C. E. Meek, and T. Chshyolkova (2008), Regional stratospheric warmings in the Pacific-Western Canada (PWC) sector during winter 2004/2005: Implications for temperatures, winds, chemical constituents and the characterization of the Polar vortex, *Ann. Geophys.*, *26*, 3597–3622.

Marsh, D. R., A. K. Smith, M. G. Mlynczak, and J. M. Russell III (2006), SABER observations of the OH Meinel airglow variability near the mesopause, *J. Geophys. Res.*, *111*, A10S05, doi:10.1029/2005JA011451.

Mertens, C. J., M. G. Mlynczak, M. Lopez-Puertas, P. P. Wintersteiner, R. H. Picard, J. R. Winick, L. L. Gordley, and J. M. Russell III (2001), Retrieval of mesospheric and lower thermospheric kinetic temperature from measurements of $CO2$ 15-mm Earth limb emission under non-LTE conditions, *Geophys. Res. Lett.*, *28*, 1391–1394, doi:10.1029/2000GL012189.

Mertens, C. J., et al. (2004), SABER observations of mesospheric temperatures and comparisons with falling sphere measurements taken during the 2002 summer MaCWAVE campaign, *Geophys. Res. Lett.*, *31*, L03105, doi:10.1029/2003GL018605.

Mertens, C. J., et al. (2009), Kinetic temperature and carbon dioxide from broadband infrared limb emission measurements taken from the TIMED/SABER instrument, *Adv. Space Res.*, *43*, 15–27, doi:10.1016/j.asr.2008.04.017.

Mlynczak, M. G., C. J. Mertens, R. R. Garcia, and R. W. Portmann (1999), A detailed evaluation of the stratospheric heat budget: 2. Global radiation balance and diabatic circulations, *J. Geophys. Res.*, *104*, 6039–6066, doi:10.1029/1998JD200099.

Mohanakumar, K. (1994), Temperature variability over the tropical middle atmosphere, *Ann. Geophys.*, *12*, 448–496, doi:10.1007/s00585-994-0448-y.

Namboothiri, S. P., N. Sugimoto, H. Nakane, I. Matsui, and Y. Murayama (1999), Rayleigh lidar observations of temperature over Tsukuba: Winter thermal structure and comparison studies, *Earth Planets Space*, *51*, 825–832.

Nee, J. B., S. Thulasiraman, W. N. Chen, M. Venkat Ratnam, and D. Narayana Rao (2002), Middle atmospheric temperature structure over two tropical locations, Chung Li (25°N, 121°E) and Gadanki (13.4°N, 79.2°E), *J. Atmos. Sol. Terr. Phys.*, *64*, 1311–1319, doi:10.1016/S1364-6826(02)00114-1.

Parameswaran, K., et al. (2000), Altitude profiles of temperature from 4–80 km over the tropics from MST radar and lidar, *J. Atmos. Sol. Terr. Phys.*, *62*, 1327–1337, doi:10.1016/S1364-6826(00)00124-3.

Ratnam, M. V., G. K. Kumar, B. V. K. Murthy, A. K. Patra, V. V. M. J. Rao, S. V. B. Rao, K. K. Kumar, and G. Ramkumar (2008), Long-term variability of the low latitude mesospheric SAO and QBO and their relation with stratospheric QBO, *Geophys. Res. Lett.*, *35*, L21809, doi:10.1029/2008GL035390.

Remsberg, E. E., et al. (2008), Assessment of the quality of the Version 1.07 temperature-versus-pressure profiles of the middle atmosphere from TIMED/SABER, *J. Geophys. Res.*, *113*, D17101, doi:10.1029/2008JD010013.

Russell, J. M., III, M. G. Mlynczak, L. L. Gordley, J. Tansock, and R. Esplin (1999), An overview of the SABER experiment and preliminary calibration results, *Proc. SPIE Int. Soc. Opt. Eng.*, *3756*, 277–288.

She, C. Y., C. Chen, Z. Hu, J. Sherman, J. D. Vance, V. Vasoli, M. A. White, J. Yu, and D. A. Krueger (2000), Eight-year climatology of nocturnal temperature and sodium density in the mesopause region (80–105 km) over Fort Collins, CO (41N, 105 W), *Geophys. Res. Lett.*, *27*, 3289–3292, doi:10.1029/2000GL003825.

Shepherd, M., and C. Fricke-Begemann (2004), Study of the tidal variations in mesospheric temperature at low and mid latitudes from WINDII and potassium lidar observations, *Ann. Geophys.*, *22*, 1513–1528.

Siva Kumar, V., P. B. Rao, and M. Krishnaiah (2003), Lidar measurements of stratosphere-mesosphere thermal structure at a low latitude: Comparison with satellite data and models, *J. Geophys. Res.*, *108*(D11), 4342, doi:10.1029/2002JD003029.

Sridharan, S., et al. (2008), A report on long-term trends and variabilities in middle atmospheric temperature over Gadanki (13.51°N, 79.21°E), *J. Atmos. Sol. Terr. Phys.*, *71*, 1463–1470, doi:10.1016/j.jastp.2008.09.017.

Taori, A., A. Guharay, and M. J. Taylor (2007), On the use of simultaneous measurements of OH and O2 emissions to investigate wave growth and dissipation, *Ann. Geophys.*, *25*, 639–643.

Venkat Ratnam, M., D. Narayana Rao, T. Narayana Rao, M. Krishnaiah, Y. Bhavani Kumar, V. Siva Kumar, and P. B. Rao (2002), Coordinated MST radar and lidar observations for the study of mesospheric structures over a tropical station, *J. Atmos. Sol. Terr. Phys.*, *64*, 349–358, doi:10.1016/S1364-6826(01)00101-8.

Xu, J., C. Y. She, W. Yuan, C. Mertens, M. Mlynczak, and J. Russell (2006), Comparison between the temperature measurements by TIMED/SABER and lidar in the midlatitude, *J. Geophys. Res.*, *111*, A10S09, doi:10.1029/2005JA011439.

Yu, C., and F. Yi (2008), Atmospheric temperature profiling by joint Raman, Rayleigh and Fe Boltzmann lidar measurements, *J. Atmos. Sol. Terr. Phys.*, *70*, 1281–1288, doi:10.1016/j.jastp.2008.04.002.

Zhao, Y., M. J. Taylor, H.-L. Liu, and R. G. Roble (2007), Seasonal oscillations in mesospheric temperatures at low-latitudes, *J. Atmos. Terr. Phys.*, *69*, 2367–2378, doi:10.1016/j.jastp.2007.07.010.

_____

A. Guharay and P. Pant, Aryabhatta Research Institute of Observational Sciences, Manora Peak, Nainital, Uttarakhand 263129, India. (guharay@in.com)

D. Nath, National Atmospheric Research Laboratory, Gadanki, Tirupati 517112, India.

B. Pande and K. Pandey, Department of Physics, DSB Campus, Kumaun University, Nainital 263001, India.

J. M. Russell III, Center for Atmospheric Sciences, Hampton University, Hampton, VA 23668, USA.